J Mater Sci (2009) 44:4827–4833
DOI 10.1007/s10853-009-3736-9

Hydrogen-storage performance of an Mg–Ni–Fe alloy prepared by reactive mechanical grinding

Myoung Youp Song · Sung Hwan Baek · Jean-Louis Bobet · Sung Nam Kwon · Seong-Hyeon Hong

Received: 18 March 2009 / Accepted: 9 July 2009 / Published online: 24 July 2009

Abstract The 71.5%Mg–23.5%Ni–5%Fe alloy prepared by reactive mechanical grinding for 4 h does not need activation. The activated sample has the hydriding rate of 0.494 wt%/min for 5 min and absorbs 3.32 wt% for 60 min at 593 K under 1.2 MPa H_2. It has the dehydriding rate of 0.330 wt%/min for 5 min and desorbs 2.42 wt%H for 20 min at 593 K 0.1 MPa H_2. The XRD pattern of 71.5 wt%Mg–23.5 wt%Ni–5 wt%Fe after reactive mechanical grinding exhibits MgH_2 in addition to starting elements Mg, Ni, and Fe. 71.5 wt%Mg–23.5 wt% Ni–5 wt%Fe after hydriding–dehydriding cycling contains Mg, Mg_2Ni, MgO, and Fe. The reactive mechanical grinding of Mg with Ni and Fe is considered to facilitate nucleation by creating many defects on the surface and in the interior of Mg, by the additive acting as active sites for the nucleation and shorten diffusion distances of hydrogen atoms by reducing the particle size of Mg. The MgH_2 formed in the as-milled 71.5 wt%Mg–23.5 wt%Ni–5 wt%Fe alloy is considered to lead to the creation of more defects and finer particle size.

M. Y. Song (✉)
Division of Advanced Materials Engineering, Department of Hydrogen and Fuel Cells, Research Center of Advanced Materials Development, Engineering Research Institute, Chonbuk National University, 664-14 1ga Deogjindong Deogjingu, Jeonju, Jeonbuk 561-756, Republic of Korea
e-mail: songmy@chonbuk.ac.kr

S. H. Baek · S. N. Kwon
Department of Hydrogen and Fuel Cells, Chonbuk National University, 664-14 1ga Deogjindong Deogjingu, Jeonju, Jeonbuk 561-756, Republic of Korea

J.-L. Bobet
ICMCB, CNRS [UPR 9048], Université de Bordeaux 1, 33608 Pessac Cedex, France

S.-H. Hong
Powder Materials Research Center, KIMS, Korea Institute of Machinery & Materials, 66 Sangnamdong, Changwon, Kyungnam 641-010, Republic of Korea

Introduction

Magnesium has many advantages for a hydrogen storage material such as large hydrogen storage capacity (7.6 wt%), low cost, and abundance in the earth's crust. In spite of these advantages, its hydriding and dehydriding kinetics are very slow. A lot of work to ameliorate the reaction kinetics of magnesium with hydrogen has been done by alloying certain metals with magnesium [1–7], mixing metal additives with magnesium [8], or plating nickel on the surface of magnesium [9].

Huot et al. [10] increased the hydrogenation rate of magnesium by milling under hydrogen with the addition of graphite. Imamura et al. [11] improved hydrogen-sorption kinetics of magnesium by mechanical milling of graphite and magnesium with organic additives. Oelerich et al. [12], Dehouche et al. [13], and Barkhordarian et al. [14] increased the hydriding and dehydriding rates of magnesium by planetary ball milling of magnesium hydride and metal, compound, or oxide. Yavari et al. [15] improved H-sorption kinetics of MgH_2 powders by using Fe nanoparticles generated by reactive FeF_3 addition. Berlouis et al. [16] investigated the effect of additives Ti, Pd, and Zr on the rate of hydrogen desorption from MgH_2, and reported that the presence of Pd and Zr enhanced dehydriding kinetics. Dolci et al. [17] reported that Nb_2O_5 in the mixed MgH_2/Nb_2O_5 system played an active chemical role for absorption/desorption kinetics of hydrogen in magnesium hydride.

Grigorova et al. [18] reported that the addition of an intermetallic compound $V_{0.855}Ti_{0.095}Fe_{0.05}$ by mechanical alloying in an inert medium improved significantly the hydriding kinetics of magnesium. Khrussanova et al. [19] obtained a nanocomposite 85 wt%Mg–15 wt%$Mg_2Ni_{0.8}Co_{0.2}$ by mechanical alloying in inert atmosphere, and explained its hydrogen sorption properties by the catalytic effect of the intermetallic $Mg_2Ni_{0.8}Co0_{0.2}$, the existence of Ni and Co clusters on the surface, and the process of mechanical alloying.

Song et al. [20–23] increased the hydriding and dehydriding rates of Mg by mechanical alloying of Mg with Ni under Ar atmosphere. Bobet et al. [24] reported that mechanical alloying in H_2 (reactive mechanical grinding (RMG)) for a short time(2 h) is an effective way to improve strongly the hydrogen-storage properties of both magnesium and Mg + 10 wt%Co, Ni or Fe mixtures.

Mechanically alloyed 75 wt%Mg–25 wt%Ni mixture showed high hydriding and dehydriding rates, and large hydrogen storage capacity [22, 23]. Yim et al. [25] reported that Mg–23.5 wt%Ni heat-treated after melt spinning had large hydrogen-storage capacity and high hydriding rate. However, this process for sample preparation (heat treatment after melt spinning) is very complicated and time consuming. Therefore we chose a simpler process, RMG, to prepare a mixture in this work.

Addition of Fe_2O_3 prepared by spray conversion to Mg with RMG improved greatly the hydriding rate of Mg [26]. But the preparation of Fe_2O_3 prepared by spray conversion is also a complicated process. In our previous work [27], we thus purchased Fe_2O_3 to prepare a mixture with a composition 71.5 wt%Mg–23.5 wt%Ni–5 wt%Fe_2O_3. Among the studied samples 76.5 wt%Mg–23.5 wt%Ni, 71.5 wt%Mg–23.5 wt%Ni–5 wt%Fe_2O_3, and 71.5 wt%Mg–23.5 wt%Ni–5 wt% Fe_2O_3 (spray conversion), 71.5 wt%Mg–23.5 wt% Ni–5 wt%Fe_2O_3 (spray conversion) had the highest hydriding and dehydriding rates and the largest hydrogen-storage capacity, but they are not satisfactory.

Didisheim et al. [28] synthesized a hydride Mg_2FeH_6 by the reaction of atomic ratio 2:1 Mg and Fe mixture with hydrogen in an autoclave under 2.0–12.0 MPa at 723–793 K for 2–10 days. They reported that this phase had a cubic symmetry with the K_2PtCl_6-type structure and a relatively high hydrogen-storage capacity (5.4 wt%). Puszkiel et al. [29] synthesized a mixture composed of complex hydride Mg_2FeH_6 (49 wt%), magnesium hydride MgH_2 (18 wt%), and unreacted magnesium and iron via mechanical milling of a 2 Mg–Fe elemental powder mixture with a subsequent hydriding process at 673 K and 6.0 MPa for 15 h. We chose Fe as the third additive because Fe can form Mg_2FeH_6, which has a relatively high hydrogen-storage capacity, by reaction with Mg and hydrogen.

In this work, we prepared an alloy with a composition of 71.5 wt%Mg–23.5 wt%Ni–5 wt%Fe by reactive mechanical grinding, investigated its hydrogen-storage properties, and compared with those of the previously studied alloys.

Experimental details

Pure Mg powder (particle size 297–100 μm; grit 50–150 mesh, purity 99%, Fluka), Ni (~5 μm average, purity 99.9%, CERAC), and Fe (Alfa, particle size <10 μm, purity 99.5%) were used as starting materials. A mixture with the desired composition (total weight = 8 g) was mixed in a stainless steel container (with 105 hardened steel balls, total weight = 360 g) sealed hermetically. The sample to ball weight ratio was 1/45. All sample handling was performed in a glove box under Ar in order to prevent oxidation. The disc revolution speed was 250 rpm. The mill container was then filled with high purity hydrogen gas (≈1.2 MPa). The reactive mechanical grinding was performed for 4 h (milling 2 h + refilling with H_2 + milling 2 h).

The absorbed or desorbed hydrogen quantity was measured as a function of time by a volumetric method, using Sivert's type hydriding and dehydriding apparatus described previously [30]. X-ray diffraction (XRD) analysis was carried out for the as-milled particles and for the samples after hydriding–dehydriding cycling. The weight percentage of the phases in the samples was calculated by Full Proof program. The microstructures were observed by scanning electron microscopy (SEM).

Results and discussions

Figure 1 shows the variation of the H_a versus t curve with the number of cycles n for as-milled 71.5 wt%Mg–23.5 wt%Ni–5 wt%Fe at 593 K under 1.2 MPa H_2. The percentage of absorbed hydrogen H_a is expressed with respect to the sample weight. For the measurement of the curve for $n = 1$, the samples were dehydrided for 2 h in vacuum at 623 K. Before obtaining the curves after $n = 1$, measurements of dehydriding curves were performed, and then the samples were dehydrided for 2 h in vacuum at 623 K. As-milled 71.5 wt%Mg–23.5 wt%Ni–5 wt%Fe absorbs 2.33 wt% for 5 min and 2.96 wt% for 60 min at 593 K under 1.2 MPa H_2. This sample absorbs 2.47 wt% for 5 min (the hydriding rate of 0.494 wt%/min) and 3.32 wt% for 60 min at $n = 3$. The H_a versus t curves are practically the same for the first three cycles. The sample reaches near maximum experimental hydrogen-storage capacity even at the first hydriding cycle. This shows that the 71.5%Mg–23.5%Ni–5%Fe alloy prepared by reactive mechanical grinding for 4 h does not need activation.

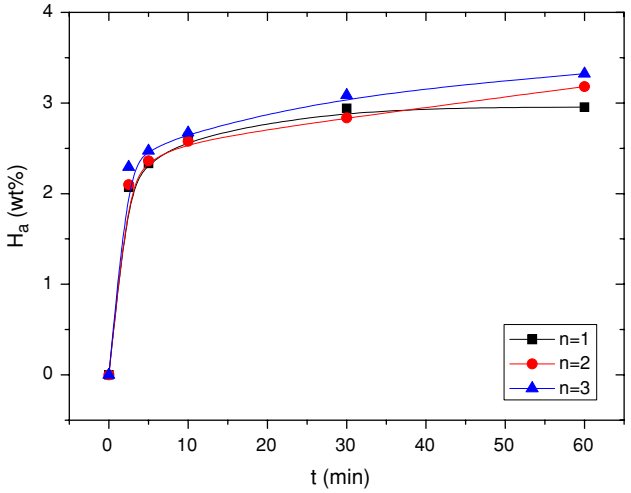

Fig. 1 Variation of the H_a versus t curve with the number of cycles for as-milled 71.5 wt%Mg–23.5 wt%Ni–5 wt%Fe at 593 K under 1.2 MPa H_2

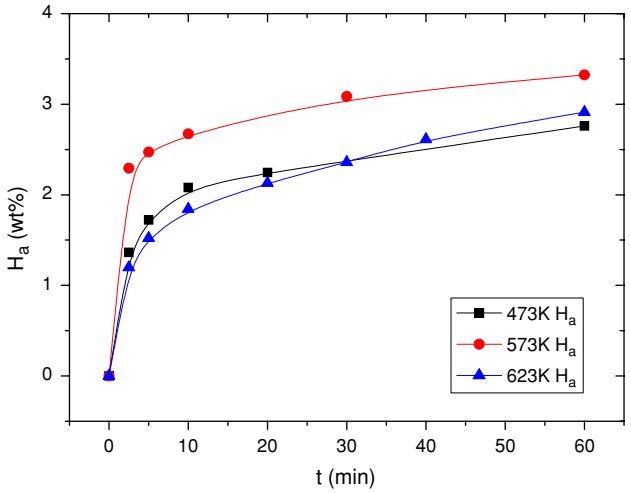

Fig. 2 Variation of the H_a versus t curve with temperature for activated 71.5 wt%Mg–23.5 wt%Ni–5 wt%Fe under 1.2 MPa H_2

Figure 2 shows the variation of the H_a versus t curve with temperature for activated 71.5 wt%Mg–23.5 wt%Ni–5 wt%Fe under 1.2 MPa H_2. As the temperature increases from 473 to 573 K, the hydriding rate increases. However, the hydriding rate decreases as the temperature increases from 573 to 623 K. This is considered to be due to the decrease in the driving force for hydriding reaction, which is related to the difference between the equilibrium plateau pressure and the applied hydrogen pressure (1.2 MPa H_2).

Figure 3 shows the variation of the H_d versus t curve with temperature for activated 71.5 wt%Mg–23.5 wt%Ni–5 wt%Fe under 0.1 MPa H_2. The percentage of desorbed hydrogen H_d is expressed with respect to the sample weight. Before obtaining these curves, the samples were

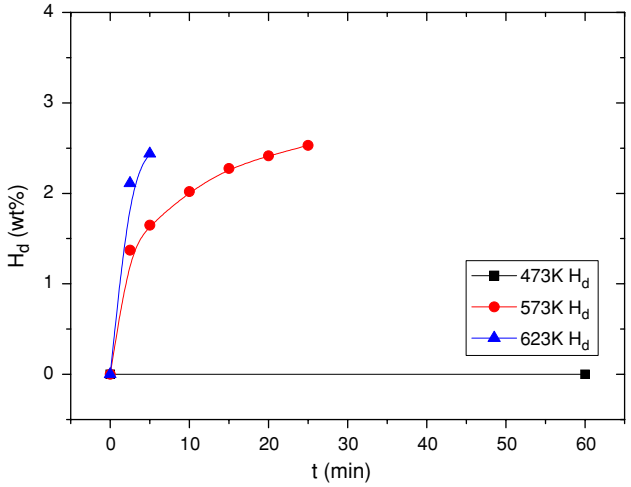

Fig. 3 Variation of the H_d versus t curve with temperature for activated 71.5 wt%Mg–23.5 wt%Ni–5 wt%Fe under 0.1 MPa H_2

hydrided for 1 h under 12 bar H_2 at experimental temperature. The sample does not desorb hydrogen at 473 K, and the dehydriding rate increases as the temperature increases from 573 to 623 K.

Figure 4 shows the microstructure of the 71.5 wt%Mg–23.5 wt%Ni–5 wt%Fe alloy after RMG at low and high magnifications. The particles of the sample are quite small and they are agglomerated.

Figure 5 shows the microstructure of the 71.5 wt%Mg–23.5 wt%Ni–5 wt%Fe alloy after hydriding–dehydriding cycling ($n = 5$) at low and high magnifications. The sample has finer particles than those after RMG. The expansion and contraction of the hydride-forming materials (Mg and Mg_2Ni) with the hydriding and dehydriding reactions is considered to make defects and cracks which can lead to the fragmentation of the particles.

Figure 6 shows the XRD pattern of 71.5 wt%Mg–23.5 wt%Ni–5 wt%Fe after reactive mechanical grinding. The sample contains MgH_2 in addition to starting elements Mg, Ni, and Fe. MgH_2 is formed by the reaction of Mg with hydrogen during reactive mechanical grinding. The weight percentages calculated by Full Proof program of MgH_2, Mg, and Ni were 28.16, 61.62, and 10.21, respectively. The Fe content was negligible.

Figure 7 shows the XRD pattern of the 71.5 wt%Mg–23.5 wt%Ni–5 wt%Fe alloy dehydrided in vacuum at $n = 5$ after activation. The sample contains Mg, Mg_2Ni, MgO, and Fe. The weight percentages calculated by Full Proof program of Mg and Mg_2Ni were 55.52 and 44.48, respectively. The MgO and Fe contents were negligible.

Figure 8 shows the XRD pattern of the 71.5 wt%Mg–23.5 wt%Ni–5 wt%Fe alloy hydrided at 593 K and 1.2 MPa ($n = 6$) after activation. The sample contains Mg, MgH_2, Mg_2NiH_4, MgO, Ni, and Fe. In the hydrided

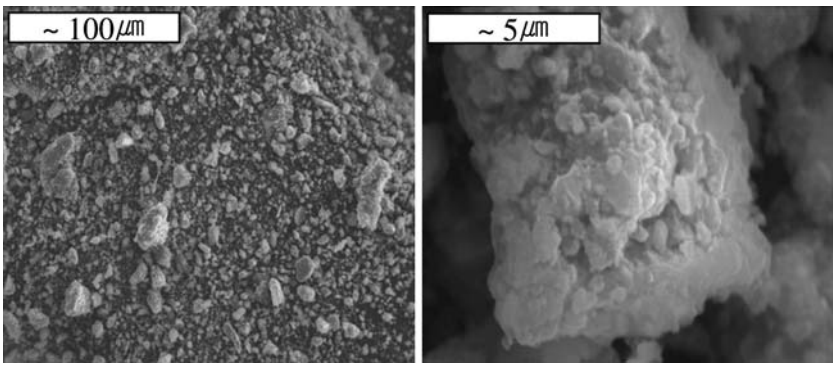

Fig. 4 Microstructure of the 71.5 wt%Mg–23.5 wt%Ni–5 wt%Fe alloy after reactive mechanical grinding at low and high magnifications

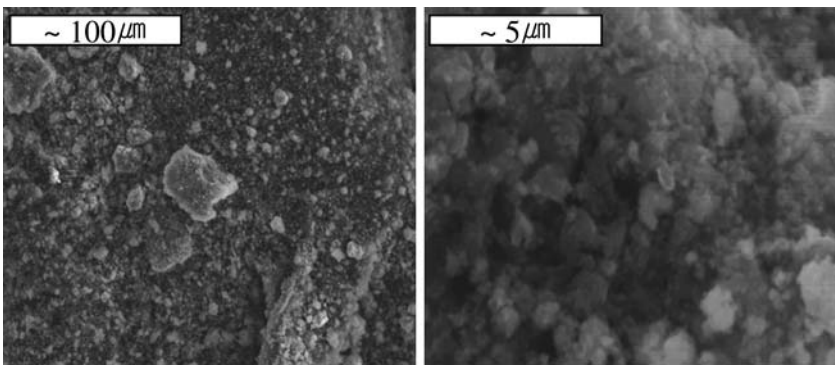

Fig. 5 Microstructure of the 71.5 wt%Mg–23.5 wt%Ni–5 wt%Fe alloy after hydriding–dehydriding cycling at low and high magnifications ($n = 5$)

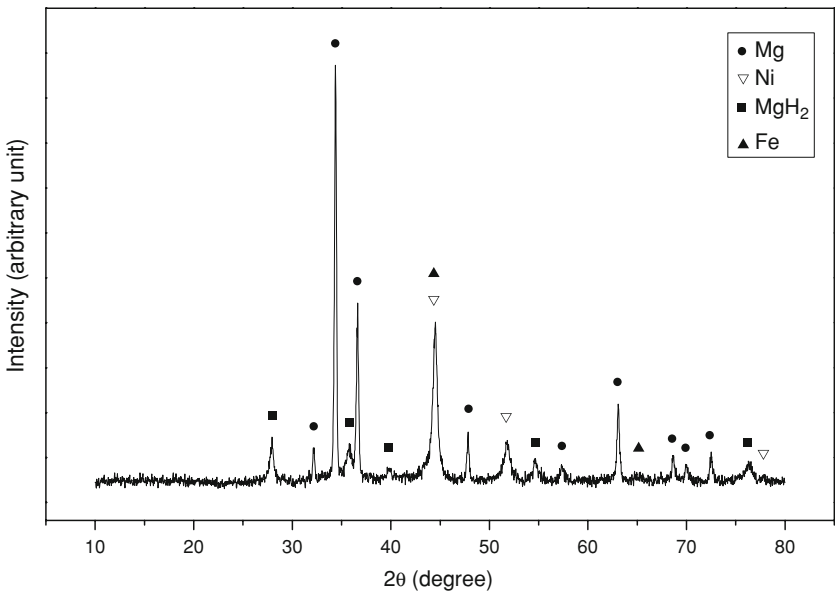

Fig. 6 XRD pattern of 71.5 wt%Mg–23.5 wt%Ni–5 wt%Fe after reactive mechanical grinding

samples, Mg_2FeH_6 phase was not detected probably because the temperature and the hydrogen pressure were not high enough for the Mg_2FeH_6 phase to form. During hydriding–dehydriding cycling, hydriding and dehydriding reactions of both Mg and Mg_2Ni phases occur under our experimental conditions.

Figure 9 shows the variation of the H_a versus t curves at 593 K 1.2 MPa H_2 at the first cycle ($n = 1$) with the samples: 76.5 wt%Mg–23.5 wt%Ni, 71.5 wt%Mg–23.5 wt%Ni–5 wt%Fe_2O_3, 71.5 wt%Mg–23.5 wt%Ni–5 wt%Fe_2O_3 (spray conversion), and 71.5 wt%Mg–23.5 wt%Ni–5 wt%Fe. 71.5 wt%Mg–23.5 wt%Ni–5 wt%Fe has the highest hydriding rate of 0.466 wt%/min for 5 min and the largest H_a value after 60 min of 2.96 wt%. The hydriding rate and the H_a value after 60 min then decrease in the order of 71.5 wt%Mg–23.5 wt%Ni–5 wt%Fe_2O_3 (spray conversion), 71.5 wt%Mg–23.5 wt%Ni–5 wt%Fe_2O_3, and 76.5 wt%Mg–23.5 wt%Ni.

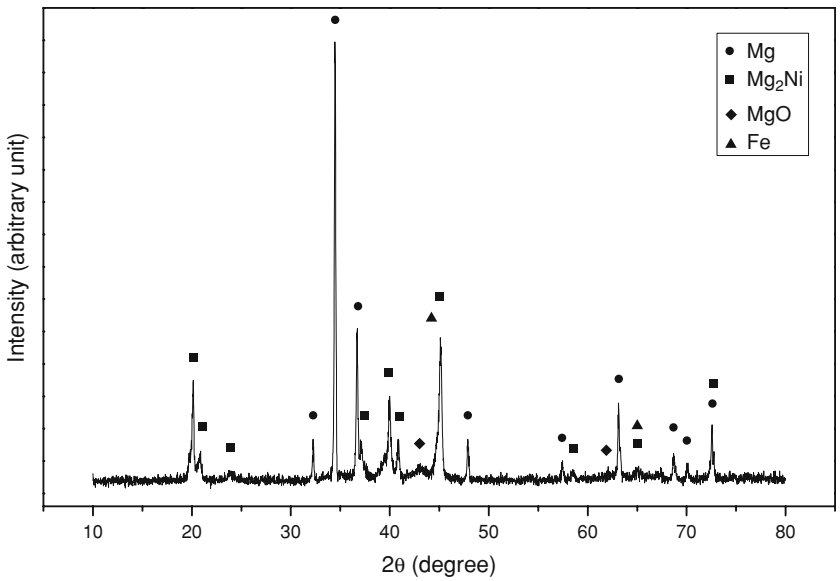

Fig. 7 XRD pattern of the 71.5 wt%Mg–23.5 wt%Ni–5 wt%Fe alloy dehydrided in vacuum at $n = 5$ after activation

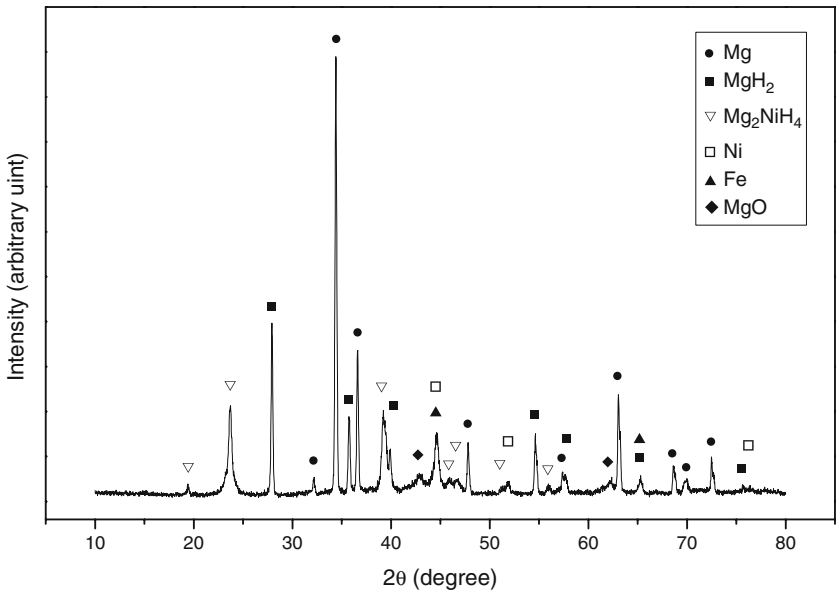

Fig. 8 XRD pattern of the 71.5 wt%Mg–23.5 wt%Ni–5 wt%Fe alloy hydrided at 593 K and 1.2 MPa ($n = 6$) after activation

Figure 10 shows the variation of the H_a versus t curves at 593 K 1.2 MPa H_2 after activation ($n = 3$) with the samples: 76.5 wt%Mg–23.5 wt%Ni, 71.5 wt%Mg–23.5 wt% Ni–5 wt% Fe_2O_3, 71.5 wt%Mg–23.5 wt%Ni–5 wt%Fe_2O_3 (spray conversion), and 71.5 wt%Mg–23.5 wt%Ni–5 wt% Fe. 71.5 wt%Mg–23.5 wt%Ni–5 wt%Fe has the highest hydriding rate of 0.494 wt%/min for 5 min and the largest H_a value after 60 min of 3.32 wt%. The hydriding rate and the H_a value after 60 min then decrease in the order of 71.5 wt%Mg–23.5 wt%Ni–5 wt%Fe_2O_3 (spray conversion), 71.5 wt%Mg–23.5 wt%Ni–5 wt%Fe_2O_3, and 76.5 wt% Mg–23.5 wt%Ni.

Figure 11 shows the variation of the H_d versus t curves at 593 K 0.1 MPa H_2 after activation ($n = 3$) with the samples: 76.5 wt%Mg–23.5 wt%Ni, 71.5 wt%Mg–23.5 wt% Ni–5 wt%Fe_2O_3, 71.5 wt%Mg–23.5 wt%Ni–5 wt%Fe_2O_3 (spray conversion), and 71.5 wt%Mg–23.5 wt%Ni–5 wt% Fe. 71.5 wt%Mg–23.5 wt%Ni–5 wt%Fe has the highest dehydriding rate of 0.330 wt%/min for 5 min and the largest H_d value after 20 min of 2.42 wt%. The dehydriding ?tul?> rate and the H_d value after 20 min then decrease in the order of 71.5 wt%Mg–23.5 wt%Ni–5 wt%Fe_2O_3 (spray conversion), 71.5 wt%Mg–23.5 wt%Ni–5 wt% Fe_2O_3, and 76.5 wt%Mg–23.5 wt%Ni.

Song [20] reviewed the kinetic studies of the hydriding and the dehydriding reactions of Mg. Many works do not agree with one another on the rate-controlling step(s) for hydriding or dehydriding of magnesium. However, there is no contradiction in the points that the hydriding and dehydriding reactions of Mg are nucleation-controlled under

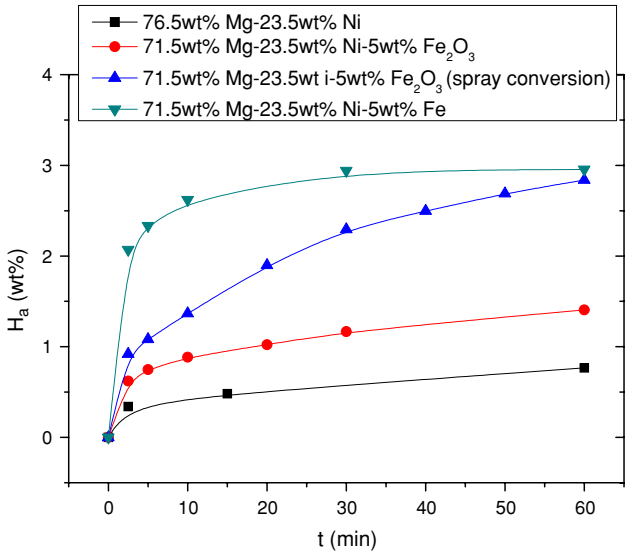

Fig. 9 Variation of the H_a versus t curves at 593 K 1.2 MPa H_2 at the first cycle ($n = 1$) with the samples: 76.5 wt%Mg–23.5 wt%Ni, 71.5 wt%Mg–23.5 wt%Ni–5 wt%Fe_2O_3, 71.5 wt%Mg–23.5 wt%Ni–5 wt%Fe_2O_3 by spray conversion, and 71.5 wt%Mg–23.5 wt%Ni–5 wt%Fe

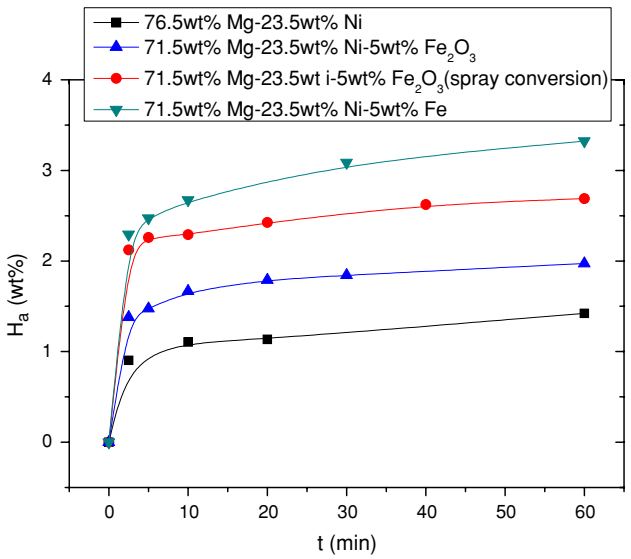

Fig. 10 Variation of the H_a versus t curves at 593 K 1.2 MPa H_2 after activation ($n = 3$) with the samples: 76.5 wt%Mg–23.5 wt%Ni, 71.5 wt%Mg–23.5 wt%Ni–5 wt% Fe_2O_3, 71.5 wt%Mg–23.5 wt%Ni–5 wt%Fe_2O_3 by spray conversion, and 71.5 wt%Mg–23.5 wt%Ni–5 wt%Fe

certain conditions and progress by a mechanism of nucleation and growth, and that the hydriding rates of Mg are controlled by the diffusion of hydrogen through a growing Mg hydride layer.

The variation of H_a absorbed by pure Mg after reactive mechanical grinding at 593 K under 1.2 MPa H_2 with time t was studied according to the number of cycles n. The pure Mg after reactive mechanical grinding absorbed small

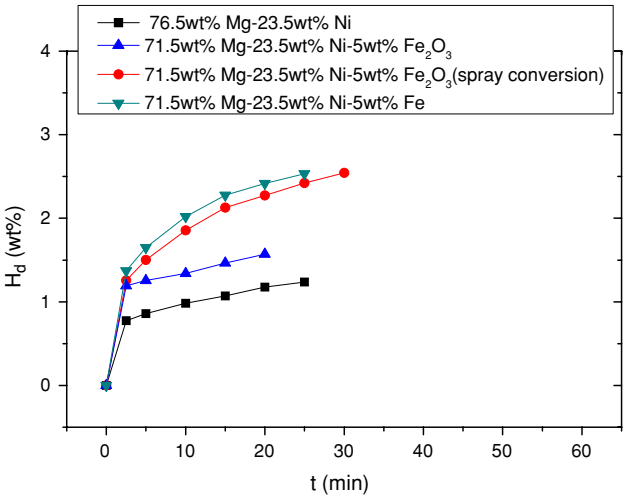

Fig. 11 Variation of the H_d versus t curves at 593 K 0.1 MPa H_2 after activation ($n = 3$) with the samples: 76.5 wt%Mg–23.5 wt%Ni, 71.5 wt%Mg–23.5 wt%Ni–5 wt%Fe_2O_3, 71.5 wt%Mg–23.5 wt%Ni–5 wt%Fe_2O_3 by spray conversion, and 71.5 wt%Mg–23.5 wt%Ni–5 wt%Fe

quantity of hydrogen ($H_a = 0.45$ wt%H after 60 min at $n = 1$) and its hydriding rate decreased as the number of cycles increased. The decrease in hydriding rate of this sample with cycling is considered due to the difficulty of the decomposition of Mg hydride during dehydriding of the previous cycle and the sintering of Mg particles during hydriding–dehydriding cycling. The as-milled 71.5 wt% Mg–23.5 wt%Ni–5 wt%Fe absorbed 2.33 wt% for 5 min and 2.96 wt% for 60 min.

The RMG of Mg with Ni and Fe is considered to facilitate nucleation by creating many defects on the surface and in the interior of Mg, by the additive acting as active sites for the nucleation, and shorten diffusion distances of hydrogen atoms by reducing the particle size of Mg.

The MgH_2 phase formed in the as-milled 71.5 wt%Mg–23.5 wt%Ni–5 wt%Fe alloy. On the other hand, it did not form in the as-milled 76.5 wt%Mg–23.5 wt%Ni, 71.5 wt% Mg–23.5 wt%Ni–5 wt%Fe_2O_3, and 71.5 wt%Mg–23.5 wt% Ni–5 wt%Fe_2O_3 (spray conversion) alloys. The MgH_2 phase, which is brittle, formed in the as-milled 71.5 wt% Mg–23.5 wt%Ni–5 wt%Fe alloy is considered to lead to the creation of more defects and the finer particle size. This is considered to bring about the higher hydriding and dehydriding rates, and the larger hydrogen-storage capacity of the 71.5 wt%Mg–23.5 wt%Ni–5 wt%Fe alloy than the other alloys.

Created defects and cracks, and the fragmentation into fine particles, due to the expansion and contraction of the hydride-forming materials (Mg and Mg_2Ni) with the hydriding and dehydriding reactions, are also considered to increase the higher hydriding and dehydriding rates of the alloys.

Oelerich et al. [12], Dehouche et al. [13], and Barkhordarian et al. [14] improved hydrogen-sorption kinetics by planetary ball milling of magnesium hydride and metal, compound, or oxide. The initial MgH_2 powder was pre-milled for 20 h and the additive was then added in the desired overall ratio, and milled for a further 100 h. The magnesium mixtures prepared by them showed the higher hydriding and dehydriding rates than the mixture of this work. However, their starting materials are different from ours. They used the magnesium hydride while we used the pure magnesium as starting materials. They pre-milled for 20 h and then milled for a further 100 h, while we milled for 4 h.

Conclusions

As-milled 71.5 wt%Mg–23.5 wt%Ni–5 wt%Fe at 593 K under 1.2 MPa H_2 absorbs 2.33 wt% for 5 min and 2.96 wt% for 60 min. At the third cycle, the sample has the hydriding rate of 0.494 wt%/min for 5 min and absorbs 3.32 wt% for 60 min at 593 K under 1.2 MPa H_2, and it has the dehydriding rate of 0.330 wt%/min for 5 min and desorbs 2.42 wt%H for 20 min at 593 K 0.1 MPa H_2. The 71.5%Mg–23.5%Ni–5%Fe alloy prepared by reactive mechanical grinding for 4 h does not need activation. The XRD pattern of 71.5 wt%Mg–23.5 wt%Ni–5 wt%Fe after reactive mechanical grinding exhibits MgH_2 in addition to starting elements Mg, Ni, and Fe. 71.5 wt%Mg–23.5 wt% Ni–5 wt%Fe after hydriding–dehydriding cycling contains Mg, Mg_2Ni, MgO, and Fe. The reactive mechanical grinding of Mg with Ni and Fe is considered to facilitate nucleation by creating many defects on the surface and in the interior of Mg, by the additive acting as active sites for the nucleation, and shorten diffusion distances of hydrogen atoms by reducing the particle size of Mg. The MgH_2 formed in the as-milled 71.5 wt%Mg–23.5 wt%Ni–5 wt%Fe alloy is considered to lead to the creation of more defects and the finer particle size.

Acknowledgement This research was performed for the Hydrogen Energy R&D Center, one of the twenty-first century Frontier R&D Program, funded by the Ministry of Science and Technology.

References

1. Reilly JJ, Wiswall RH (1967) Inorg Chem 6(12):2220
2. Reilly JJ, Wiswall RH Jr (1968) Inorg Chem 7(11):2254
3. Mintz MH, Gavra Z, Hadari Z (1978) J Inorg Nucl Chem 40:765
4. Pezat M, Hbika A, Darriet B, Hagenmuller P (1978) French Anvar Patent 78 203 82
5. Pezat M, Hbika A, Darriet B, Hagenmuller P (1979) Mater Res Bull 14:377
6. Pezat M, Darriet B, Hagenmuller P (1980) J Less-Common Met 74:427
7. Akiba E, Nomura K, Ono S, Suda S (1982) Int J Hydrogen Energy 7(10):787
8. Tanguy B, Soubeyroux JL, Pezat M, Portier J, Hagenmuller P (1976) Mater Res Bull 11:1441
9. Eisenberg FG, Zagnoli DA, Sheridan JJ III (1980) J Less-Common Met 74:323
10. Huot J, Tremblay M-L, Schulz R (2003) J Alloys Compd 356–357:603
11. Imamura H, Kusuhara M, Minami S, Matsumoto M, Masanari K, Sakata Y, Itoh K, Fukunaga T (2003) Acta Mater 51(20):6407
12. Oelerich W, Klassen T, Bormann R (2001) J Alloys Compd 322:L5
13. Dehouche Z, Klassen T, Oelerich W, Goyette J, Bose TK, Schulz R (2002) J Alloys Compd 347:319
14. Barkhordarian G, Klassen T, Bormann R (2003) Scr Mater 49:213
15. Yavari AR, LeMoulec A, de Castro FR, Deledda S, Friedrichs O, Botta WJ, Vaughan G, Klassen T, Fernandez A, Kvick A (2005) Scr Mater 52(8):719
16. Berlouis LEA, Honnor P, Hall PJ, Morris S, Dodd SB (2006) J Mater Sci 41(19):6403. doi:10.1007/s10853-006-0732-1
17. Dolci F, Di Chio M, Baricco M, Giamello E (2007) J Mater Sci 42(17):7180. doi:10.1007/s10853-007-1567-0
18. Grigorova E, Khristov M, Khrussanova M, Peshev P (2008) J Mater Sci 43(15):5336. doi:10.1007/s10853-008-2779-7
19. Khrussanova M, Mandzhukova T, Grigorova E, Khristov M, Peshev P (2007) J Mater Sci 42(10):3338. doi:10.1007/s10853-006-0586-6
20. Song MY (1995) J Mater Sci 30:1343. doi:10.1007/BF00356142
21. Song MY, Ivanov EI, Darriet B, Pezat M, Hagenmuller P (1985) Int J Hydrogen Energy 10(3):169
22. Song MY, Ivanov EI, Darriet B, Pezat M, Hagenmuller P (1987) J Less-Common Met 131:71
23. Song MY (1995) Int J Hydrogen Energy 20(3):221
24. Bobet J-L, Akiba E, Nakamura Y, Darriet B (2000) Int J Hydrogen Energy 25:987
25. Yim CD, You BS, Na YS, Bae JS (2007) Catal Today 120:276
26. Song MY, Kwon IH, Kwon SN, Park CG, Hong SH, Mumm DR, Bae JS (2006) J Alloys Compd 415:266
27. Baek SH (2009) Improvement of the hydrogen-storage properties of Mg by the addition of Ni, Fe and Fe_2O_3 and reactive mechanical grinding. M. Eng. Thesis, Chonbuk National University, Republic of Korea
28. Didisheim JJ, Zolliker P, Yvon K, Fischer P, Schefer J, Gubelmann M, Williams AF (1984) Inorg Chem 23:1953
29. Puszkiel JA, Arneodo Larochette P, Gennari FC (2008) Int J Hydrogen Energy 33:3555
30. Song MY, Ahn DS, Kwon IH, Ahn HJ (1999) Met Mater Int 5(5):485